

**Electronic reconstruction at a buried ionic-covalent interface driven by surface reactions**

C.-T. Lou (羅中廷), H.-D. Li (李宏道), J.-Y. Chung (鐘仁陽), and D.-S. Lin (林登松)\*,†

*Department of Physics, National Tsing Hua University, 101 Section 2 Kuang Fu Road, Hsinchu 30013, Taiwan  
and Institute of Physics, National Chiao-Tung University, 1001 Ta-Hsueh Road, Hsinchu 30010, Taiwan*

T.-C. Chiang (江台章)\*,‡

*Department of Physics, University of Illinois, 1110 West Green Street, Urbana, Illinois 61801-3080, USA  
and Frederick Seitz Materials Research Laboratory, University of Illinois, 104 South Goodwin Avenue, Urbana, Illinois 61801-2902, USA  
(Received 11 September 2009; revised manuscript received 11 October 2009; published 13 November 2009)*

Lattice-matched ionic NaCl films were grown layer by layer on covalent Ge(100) using cycles of two half reactions (HRs) that involved the alternative adsorption of Cl and Na. The Ge *3d* photoemission spectra obtained after full cycles of growth resembled that of clean Ge(100), but came to resemble that of the polar Cl-terminated surface after the subsequent half reaction of Cl adsorption. Concurrently, the Na and Cl core levels of the nanofilms shifted by  $\sim 1.7$  eV between these two interface configurations. Our results demonstrate that reactions on the NaCl surface drive periodic electronic reconstructions at the NaCl-Ge interface.

DOI: [10.1103/PhysRevB.80.195311](https://doi.org/10.1103/PhysRevB.80.195311)

PACS number(s): 68.35.Fx, 79.60.-i, 81.15.Aa, 82.65.+r

**I. INTRODUCTION**

Ultrathin dielectric, metallic, and molecular films play a critical role in nanoscale science and technology.<sup>1-4</sup> Coupling of the atomic and electronic structures between the interface and surface of subnanometer-thick films is an important issue, yet an interface or surface is not typically expected to be influenced by and/or to significantly affect chemical reactions and electronic properties on the other side of the film. A few exceptional cases exist: Surnev *et al.*,<sup>5</sup> in a study of the growth in vanadium oxides on Pd(111), reported layer-dependent structures and oscillatory oxidation states. Quek *et al.*<sup>6</sup> found the adsorption of O<sub>2</sub> on Au films on top of TiO<sub>2</sub>-coated Mo(112) to depend on the induced charge redistribution at the Au-TiO<sub>2</sub> interface. Olmstead *et al.*<sup>7</sup> reported a large core-level shift at the interface of a four-layer CaF<sub>2</sub> film grown on Si(111) after a massive exposure of the system to O<sub>2</sub>, humid N<sub>2</sub>, or humid air at atmospheric pressure; the shift was attributed to an increase in the interfacial bond length. In this paper, we report the discovery of a much more dramatic effect under a well-controlled experimental condition—periodic switching of the electronic structure and bonding character at a buried interface during the cyclic growth in a thin ionic film.

Specifically, this work investigates the formation and evolution of interfacial bonding in NaCl growth on Ge(100). The choice of NaCl is partially motivated by its prototypical ionic behavior and its close lattice matching with Ge (5.63 vs 5.65 Å). In addition, NaCl can be grown on Ge(100) layer by layer in cycles of sequential half reactions (HRs) that involve the adsorption of Cl (Cl-HR) and Na (Na-HR). This process is unlike the typical growth in alkali halides that is based on molecular-beam epitaxy (MBE) using ionically balanced molecular units.<sup>8-10</sup> The sequential HRs in this case yield additional information;<sup>11</sup> the buried interface exhibits large oscillations of bonding character (van der Waals vs ionic) that are governed by whether the growing film is ionically balanced or contains an extra layer of Cl. Therefore, film growth in our case, as a surface event, exerts a long-

range influence on the chemistry of the interface.

**II. EXPERIMENTAL DETAIL**

Our photoemission experiments were conducted at National Synchrotron Radiation Research Center in Taiwan, using a hemispherical analyzer. The Ge(100) substrates, of size  $3 \times 10$  mm<sup>2</sup>, were cut from commercial Sb-doped wafers. Each substrate underwent cycles of Ar ion sputtering and annealing to  $\sim 1000$  K for 60 s to yield a clean surface. NaCl was grown with the sample at near room temperature. To deposit Cl, the sample was exposed to a beam of Cl<sub>2</sub> gas;

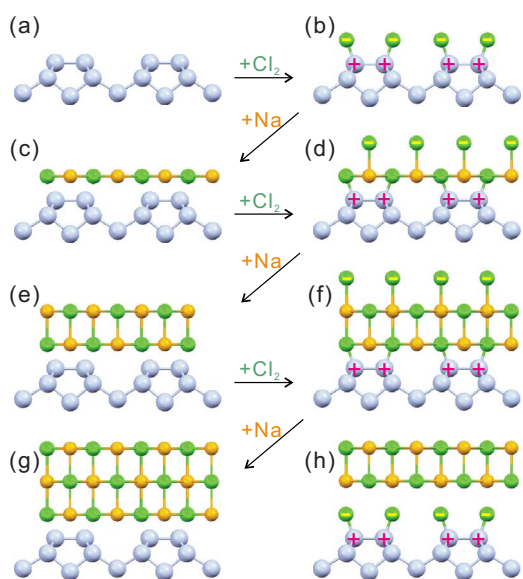


FIG. 1. (Color online) (a)–(g) Simplified models for various stages of growth in NaCl on Ge(100). The smallest, the middle, and the the largest spheres represent Na, Cl, and Ge, respectively. Some of the atoms are marked with positive and negative signs to indicate their nominal ionic states. (h) Alternate model to (f), obtained after the growth of two full layers of NaCl and an extra Cl-HR.

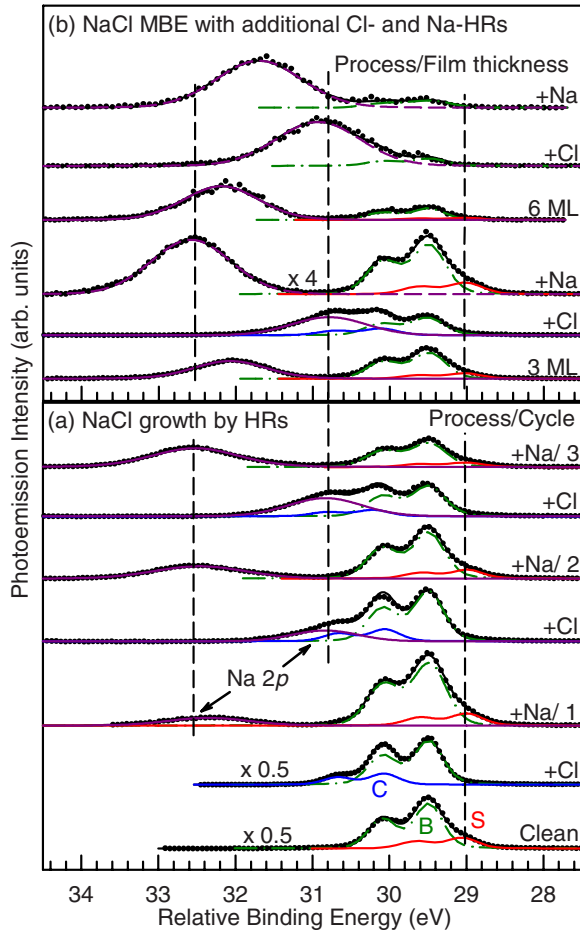


FIG. 2. (Color online) Ge 3*d* and Na 2*p* core-level photoemission spectra obtained in various stages of growth. The photon energy used was 140 eV. The Ge 3*d* line shapes are decomposed by fitting into bulk (b), surface (s), and chemically shifted (c) components. The relative binding energies refer to the Ge 3*d*<sub>5/2</sub> bulk position (29.5 eV). The vertical dashed lines highlight the periodic appearance and disappearance of the Ge 3*d* S component as well as the periodic shifts in the Na 2*p* energy.

the surface uptake of Cl was self-limiting.<sup>12</sup> Na was deposited from an SAES getter source, and the rate of deposition was determined by monitoring the change in the work function of a Si(100) test sample and the rise of a second Na 2*p* peak above a monolayer (ML) of Na.<sup>13,14</sup> For comparison, the growth in NaCl by MBE was also investigated. This growth was performed by thermal evaporation of NaCl at a deposition rate of  $\sim 1$  Å/min, as measured using a flux monitor, which was calibrated against the photoemission signal. In the following, the film thickness is specified in terms of the site density of the Ge(100)-(1 × 1) surface: one monolayer (ML) =  $6.24 \times 10^{14}$  atoms/cm<sup>2</sup>.

### III. RESULTS AND DISCUSSION

Figure 1 schematically depicts sample configurations in various stages of deposition. The clean Ge(100) surface consists of dimer rows; each surface atom has a dangling bond.<sup>15,16</sup> Exposure to Cl<sub>2</sub> until saturation yields a Cl-

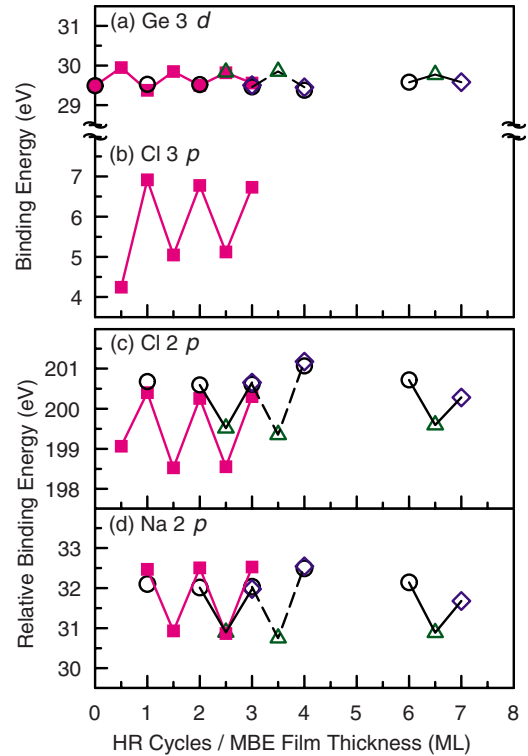


FIG. 3. (Color online) Binding energies referred to the Fermi level and relative binding energies referred to the Ge 3*d*<sub>5/2</sub> B component position (29.5 eV relative to the valence-band maximum) for various core levels as indicated at different stages of NaCl growth. Data for films grown by HRs and MBE are shown in magenta-filled squares and black circles, respectively, while data obtained after an additional Cl-HR and Na-HR on top of MBE films are shown in green triangles and blue diamonds, respectively.

terminated (2 × 1) surface.<sup>16</sup> Further exposure of the surface to one ML of Na results in a stoichiometric NaCl(100) ML, as shown in Fig. 1(c). A (100) plane in the NaCl structure has interlocked square lattices of Na and Cl, with no net dipole moment. First-principles calculations show that the first monolayer of NaCl on Ge(100) is somewhat buckled, but this bulking declines in two ML and thicker films.<sup>17</sup> The process of sequential Cl and Na HRs was repeated to establish a film, as displayed in Figs. 1(a)–1(g).

Figure 2(a) presents Ge 3*d* and Na 2*p* core-level spectra. The Ge 3*d* spectrum of the clean surface shows a bulk component (B) and a surface-shifted (−0.44 eV) component (S); the latter is associated with the Ge atoms in the top layer.<sup>16,18</sup> Here, the relative binding-energy scale is referenced to the bulk Ge 3*d*<sub>5/2</sub> position (29.5 eV relative to the valence-band maximum). This energy-referencing scheme eliminates any shifts due to changes in band bending. Figure 3(a) shows the measured binding energy of the Ge 3*d*<sub>5/2</sub> B component relative to the Fermi level at various stages of sample growth; it varies by  $\sim 0.34$  eV due to changes in surface band bending.

Upon Cl termination, the S component is replaced by a chemically shifted component (C) due to bonding to the Cl.<sup>12,16,18</sup> The chemical shift of +0.58 eV from the bulk suggests that the top Ge layer is positively charged (Ge<sup>+</sup>).<sup>19</sup> When a Na ML is added, the C component is eliminated, and

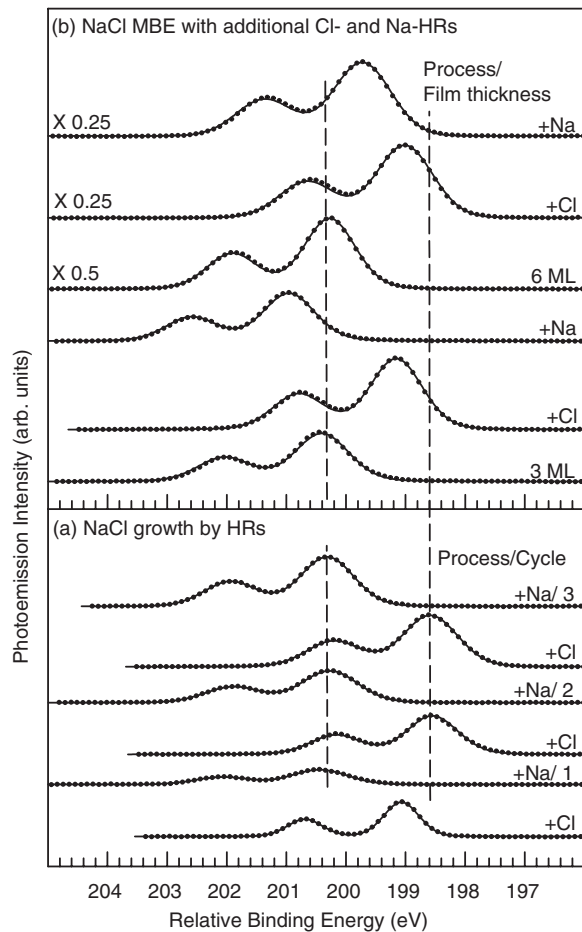


FIG. 4. Spectra of Cl  $2p$  corresponding to those of Na  $2p$  and Ge  $3d$  in Fig. 2, using the same relative scale of binding energy. The photon energy used was 240 eV. Circles represent data, and solid curves are fitted. Vertical dashed lines emphasize the periodic shifts in core levels.

the S component reappears. The line shape becomes clean-Ge(100)-like, suggesting a very weak bonding between the ionically balanced NaCl ML and the Ge(100) surface. A weak Na  $2p$  core level is observed at  $\sim 3$  eV on the higher binding-energy side of the B component of Ge  $3d$ . The next Cl-HR restores the C component of Ge  $3d$  and shifts the Na  $2p$  core level by about  $-1.5$  eV into a position that partially overlaps the Ge  $3d$  peaks. Adding another Na ML reverses these changes: the Na  $2p$  returns to the high-binding-energy position and the Ge  $3d$  line shape becomes clean-surface-like again. These oscillatory variations are repeated in subsequent HR steps. Notably, the Na  $2p$  line shape shows a single component at each step of the growth; a mixture with two or more well-separated binding energies was never observed.<sup>14</sup> Accordingly, the core-level shift is a collective effect that involves the Na atoms in all layers; the results point to an overall shift in electrostatic potential throughout the film.

For comparison, the bottom spectrum in Fig. 2(b) is obtained after the growth of three ML NaCl by MBE. It is similar to that obtained after repeated cycles of HRs for the same total coverage. The Na  $2p$  energies differ by about 0.46 eV, but this difference is much less than the oscillatory shifts

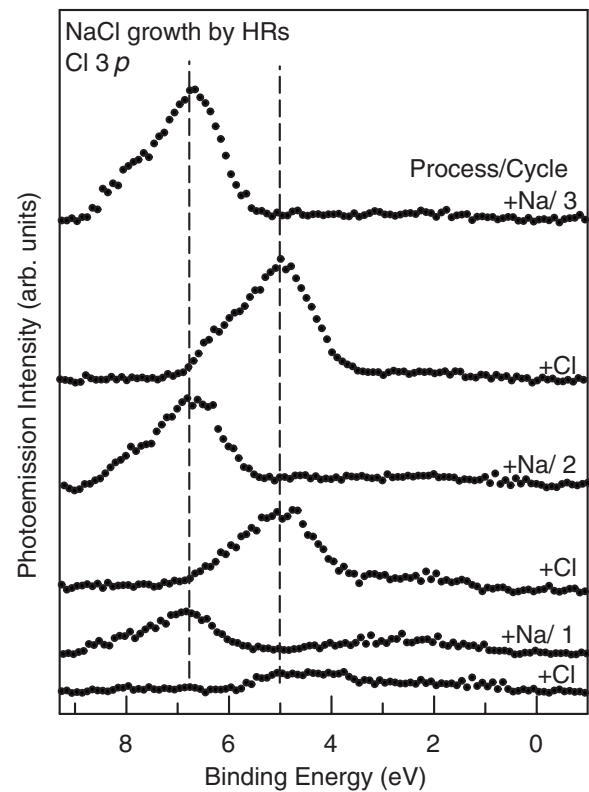


FIG. 5. Spectra of the Cl  $3p$  level corresponding to those of Na  $2p$  and Ge  $3d$  in Fig. 2(a). The binding energies are referred to the Fermi level. The photon energy used was 140 eV. Vertical dashed lines emphasize the periodic shifts.

of  $\sim 1.7$  eV during HR growth. The Na  $2p$  core level of MBE films commonly varied in energy by a fraction of one eV probably because of defects, roughness, or the departure in stoichiometry that is caused by thermal decomposition of the NaCl evaporant. A Cl-HR was then conducted on this three ML MBE film, followed by a Na-HR. The oscillation of the Na  $2p$  binding energy was again observed, and the line shape of the Ge  $3d$  switched from clean-surface-like to Cl-termination-like, and then back. The trend continued for higher coverages, but with reduced energy shifts, as displayed in Fig. 2(b), which presents the separate results after a Cl-HR and a Na-HR atop a six ML MBE film.

The spectra of the Cl  $2p$  core level corresponding to those of Na  $2p$  and Ge  $3d$  in Fig. 2 are displayed in Fig. 4 in the same order. The results reveal oscillatory shifts in binding energy just as those in the Na  $2p$  case. The Cl  $2p$  takes on a high-binding-energy position for the stoichiometric NaCl films and a low-binding-energy position for the films with an excess layer of Cl atop. The difference in binding energy is  $\sim 1.7$  eV for films that are built up entirely by HRs, and somewhat lower for thicker films that are prepared by an additional cycle of two HRs on top of MBE films.

Figures 3(c) and 3(d) summarize observed core-level shifts versus the number of deposition cycles. Evidently, the Na  $2p$  and Cl  $2p$  shift in unison. Figure 3(b) depicts the shifts in the Cl  $3p$  level in the HR case. The spectra of the Cl  $3p$  level are shown in Fig. 5. Although the Cl  $3p$  is a valence level, and not a core level, its behavior follows

closely that of the Cl  $2p$  core level. This similarity is expected, since the Cl  $3p$  level is nominally filled, and its energy should approximately track the local electrostatic potential in the same manner as the core levels.

Large chemical shifts can occur during interface formation or surface adsorption when ionic bonding causes charge transfer and a corresponding shift in electrostatic potential.<sup>7,20–24</sup> However, the observation herein of large oscillatory shifts in the core levels of both the cations and the anions in a film that is grown to many MLs is novel. Since the band gap of Ge is just 0.66 eV at room temperature, our observed core-level shifts of  $\sim 1.7$  eV are much larger and cannot possibly be explained by the effect of band bending. The correlated oscillations of the Na  $2p$ , Cl  $2p$ , and Cl  $3p$  energies for all atomic layers in the film suggest that these shifts must be derived from variations in electrostatic potential at the interface.

The above-mentioned results may be explained in terms of two bonding states, A and B, at the NaCl-Ge interface. State A is associated with a stoichiometric NaCl film; the interface bonding is so weak that even the surface-shifted Ge  $3d$  core-level component in a clean Ge(100) surface is hardly affected by the overlayer. Apparently, the strong ionic bonding between Na and Cl leaves the NaCl film in a low-energy state, rendering it inert and largely noninteracting with the Ge substrate.<sup>10,17</sup> Since each (100) plane in the NaCl structure is ionically balanced with no net dipole, the resulting interfacial bonding is likely of the van der Waals-type with an insignificant dipole moment at the interface.

Bonding state B is associated with films with an extra layer of Cl atop the stoichiometric NaCl layer, as indicated in Figs. 1(d) and 1(f). The Ge  $3d$  line shapes in this state resemble that of the Cl-terminated Ge(100) surface. The presence of the component C of Ge  $3d$  suggests a very similar type of ionic bonding with a positively charged Ge<sup>+</sup> layer at the interface. The schematic model in Fig. 1(f) suggests that the outermost Cl layer is negatively charged as the whole system must be electrically neutral. However, such a Cl<sup>-</sup>-Ge<sup>+</sup> ionic charge separation over a large distance is unlikely, because it would store a large electrostatic energy and is also inconsistent with the experimental results, since the electric

field associated with such charge separation would cause different core-level shifts for the various NaCl layers in the film. Figure 1(h) depicts an idealized scenario that is entirely consistent with the experimental results. In this picture, the Ge(100) surface is terminated by Cl, and the remaining NaCl forms an “inert” capping layer. The interface dipole that is associated with the ionic bonding gives rise to the overall core-level shifts in the NaCl film. This configuration requires substantial reorganization of the NaCl structure upon a Cl-HR and may seem unlikely. However, the large electric field that is associated with the naïve model in Fig. 1(f) potentially drives ionic motion or lattice distortion,<sup>25</sup> producing a final system configuration that is close to the ideal model shown in Fig. 1(h). Upon a Cl-HR, a thick NaCl film can relax in other ways, possibly explaining the gradual reduction in the core-level shifts as the thickness of the films increases.

#### IV. CONCLUSIONS

A surprisingly electronic reconstruction at a buried NaCl-Ge(100) interface is observed during cyclic half reactions. Periodic switching between ionic bonding and van der Waals bonding at the interface is evident from the measured core-level shifts. The large long-range chemical and electronic coupling can be attributed to a strong electrostatic interaction associated with the high ionicity of NaCl. The implication that lattice distortions or ionic motions minimize the electric-field energy during the alternative adsorption of anions and cations suggests an interesting avenue for materials engineering. The findings in this investigation may have important implications for nanomaterials and devices with dielectric-covalent junctions.

#### ACKNOWLEDGMENTS

This work is supported by the National Science Council of Taiwan (Contract No. NSC 95-2112-M007-067-MY4 for D.S.L.) and the U.S. Department of Energy (Grant No. DE-FG02-07ER46383 for T.C.C.). We wish to thank S. F. Tsai and S. Gwo for helpful discussions.

\*Author to whom correspondence should be addressed.

†dslin@phys.nthu.edu.tw

‡tcchiang@illinois.edu

<sup>1</sup>F. E. Olsson, S. Paavilainen, M. Persson, J. Repp, and G. Meyer, *Phys. Rev. Lett.* **98**, 176803 (2007).

<sup>2</sup>M. S. Chen and D. W. Goodman, *Science* **306**, 252 (2004).

<sup>3</sup>R. Balog, P. Cicman, N. C. Jones, and D. Field, *Phys. Rev. Lett.* **102**, 073003 (2009).

<sup>4</sup>Y. Segal, J. W. Reiner, A. M. Kolpak, Z. Zhang, S. Ismail-Beigi, C. H. Ahn, and F. J. Walker, *Phys. Rev. Lett.* **102**, 116101 (2009).

<sup>5</sup>S. Surnev, G. Kresse, M. G. Ramsey, and F. P. Netzer, *Phys. Rev. Lett.* **87**, 086102 (2001).

<sup>6</sup>S. Y. Quek, C. M. Friend, and E. Kaxiras, *Surf. Sci.* **600**, 3388

(2006).

<sup>7</sup>M. A. Olmstead, *Thin Films: Heteroepitaxial Systems* (World Scientific, Singapore, 1999).

<sup>8</sup>M. Pivetta, F. Patthey, M. Stengel, A. Baldereschi, and W.-D. Schneider, *Phys. Rev. B* **72**, 115404 (2005).

<sup>9</sup>K. Glöckler, M. Sokolowski, A. Soukopp, and E. Umbach, *Phys. Rev. B* **54**, 7705 (1996).

<sup>10</sup>V. Zielasek, T. Hildebrandt, and M. Henzler, *Phys. Rev. B* **69**, 205313 (2004).

<sup>11</sup>W. Hebenstreit, M. Schmid, J. Redinger, R. Podloucky, and P. Varga, *Phys. Rev. Lett.* **85**, 5376 (2000).

<sup>12</sup>D. S. Lin, J. L. Wu, S. Y. Pan, and T. C. Chiang, *Phys. Rev. Lett.* **90**, 046102 (2003).

<sup>13</sup>C. T. Lou, Ph.D. thesis, National Chiao-Tung University, 2008.

- <sup>14</sup>Y. C. Chao, L. S. O. Johansson, and R. I. G. Uhrberg, *Phys. Rev. B* **55**, 7198 (1997).
- <sup>15</sup>Y. Yoshimoto, Y. Nakamura, H. Kawai, M. Tsukada, and M. Nakayama, *Phys. Rev. B* **61**, 1965 (2000).
- <sup>16</sup>R. D. Schnell, F. J. Himpsel, A. Bogen, D. Rieger, and W. Steinmann, *Phys. Rev. B* **32**, 8052 (1985).
- <sup>17</sup>S. F. Tsay and D. S. Lin, *Surf. Sci.* **603**, 2102 (2009).
- <sup>18</sup>A. Goldoni, S. Modesti, V. R. Dhanak, M. Sancrotti, and A. Santoni, *Phys. Rev. B* **54**, 11340 (1996).
- <sup>19</sup>G. Pourtois, M. Houssa, A. Delabie, T. Conard, M. Caymax, M. Meuris, and M. M. Heyns, *Appl. Phys. Lett.* **92**, 032105 (2008).
- <sup>20</sup>D. Schmeißer, O. Böhme, A. Yfantis, T. Heller, D. R. Batchelor, I. Lundstrom, and A. L. Spetz, *Phys. Rev. Lett.* **83**, 380 (1999).
- <sup>21</sup>C.-L. Wu, H.-M. Lee, C.-T. Kuo, S. Gwo, and C.-H. Hsu, *Appl. Phys. Lett.* **91**, 042112 (2007).
- <sup>22</sup>S. Kera, Y. Yabuuchi, H. Yamane, H. Setoyama, K. K. Okudaira, A. Kahn, and N. Ueno, *Phys. Rev. B* **70**, 085304 (2004).
- <sup>23</sup>M. A. Olmstead and R. D. Bringans, *Phys. Rev. B* **41**, 8420 (1990).
- <sup>24</sup>F. Xu, M. Vos, and J. H. Weaver, *Phys. Rev. B* **39**, 8008 (1989).
- <sup>25</sup>N. V. Zagoruiko, *Mater. Sci.* **7**, 496 (1974).